Supporting Information

Choi et al. 10.1073/pnas.1218424110

SI Text

Fluorescent Lipid Dyes Have No Effect on the Inhibition of Lipid Mixing by Large α-synuclein Oligomers. To investigate the effect of dye probes on the inhibition of lipid mixing by large α-synuclein (α-Syn) oligomers, we performed two experiments: (*i*) we varied the concentration of lipid dyes [1,1′-dioctadecyl-3,3,3′,3′-tetramethylindocarbocyanine perchlorate (DiI)/1,1′-dioctadecyl-3,3,3′,3′-tetramethylindodicarbocyanine perchlorate (DiD) pair], and (*ii*) we used another dye pair, nitrobenzoxadiazole (NBD)/rhodamine. We first varied the concentrations of both DiI and DiD from 2% to 1% and 0.5% (Fig. S4 *A*–*C*). The results show that even with the dye concentration reduced by fourfold, the extent of the inhibition was nearly the same (Fig. S4*D*). This shows that the lipid-mixing inhibition by large α-Syn oligomers is independent of the lipid dyes (DiI/DiD pair). Additionally, we used another dye pair, NBD/rhodamine. Lipid compositions for the NBD/rhodamine measurements were 1-palmitoyl-2-oleoyl-sn-glycero-3-phosphocholine (POPC):1,2-dioleoyl-sn-glycero-3-(phospho-L-serine) (DOPS):cholesterol (Chol):NBD:rhodamine = 70:7:20:1.5:1.5 for v-vesicles, and POPC:DOPS:Chol = 73:7:20 for t-vesicles. We note that, unlike the DiI/DiD pair, both NBD and rhodamine were incorporated into the same v-vesicle. The procedure for proteoliposome reconstitution was identical to that of the DiI/DiD system: 10 μM each of t- and v-vesicles was mixed together to make 55 μL of the final reaction volume at 35 °C. After more than 2,000 s of the lipid-mixing reaction, 0.1% Triton X-100 detergent solution was added to the mixture to detect the maximum intensity of NBD. The 465-nm wavelength was used to excite NBD, and the increment of fluorescence intensity at the 530-nm wavelength was recorded as the result of lipid mixing. The relative percentage of lipid mixing in the NBD/rhodamine system was calculated by dividing the NBD intensity by the maximum fluorescence intensity of NBD obtained after adding 0.1% Triton X-100 (Fig. S4*F*). The result shows that large α-Syn oligomers reduce lipid mixing of the NBD/rhodamine system with efficiency similar to that of the DiI/DiD case (Fig. S4*F*). Thus, the results show that the inhibition of lipid mixing by large α-Syn oligomers in Fig. 1 was not caused by the interaction between large α-Syn oligomers and the DiI/DiD dye pairs.

No Membrane Disruption Was Induced by Large α-Syn Oligomers. In the previous work, membrane permeabilization was induced by α-Syn aggregates when vesicles were composed of 1,2-dioleoyl-sn-glycero-3-phosphate (DOPA) or 1,2-dioleoyl-sn-glycero-3-phospho-(1'-rac-glycerol) (DOPG) (1, 2). When DOPS was used as a negatively charged lipid or the composition of neutral lipids was over 50 mol%, the permeabilization by α-Syn aggregates was not observed (2). Here, we used 73% POPC, 20% Chol, and 7% DOPS for liposomes (3). Thus, the vesicles used in this work contain less than 10% of negatively charged lipids. Under these conditions, the possibility of permeabilization by large α-Syn oligomers was expected to be low. To confirm this, we tested whether large α-Syn oligomers permeabilize proteoliposomes using the sulforhodamine B (SRB) dequenching method. We prepared vesicles containing 20 mM SRB by adding 20 mM SRB during lipid film rehydration. The procedures of extrusion and protein reconstitution were identical to those of proteoliposome doped with DiI or DiD. The lipid composition was POPC:DOPS:Chol = 73:7:20 for both t- and v-vesicles. After samples were recovered from the dialysis tube, free SRB dyes were removed using Sepharose CL-4B resin (Sigma). To test membrane disruption by large α-Syn oligomers, we added 170 nM large α-Syn oligomers to 10 μM t-vesicles, v-vesicles, and protein-free vesicles, respectively. Then, the fluorescent emissions of SRB were monitored (the 532-nm wavelength excitation and the 580-nm wavelength detection) (Fig. S5). We observed that the dequenching of SRB, which is the result of membrane disruption, was nearly negligible for all types of vesicles (Fig. S5). We measured the maximum intensity of SRB by adding 0.1% Triton X-100 for each measurement.

Coflotation Assay for Measuring the Binding Properties of Large α-Syn Oligomers. We measured the binding properties of large α-Syn oligomers to proteoliposomes (t- and v-vesicles) and protein-free vesicles using the coflotation assay. Each vesicle (100 μM) was incubated with 170 nM large α-Syn oligomers for 30 min at room temperature, then the equal volume of histodenz [80% (wt/vol) solution] was added to the mixture. The sample was moved to a thick-wall centrifugation tube (Beckman), then 300 μL of 30% (wt/vol) histodenz and 100 μL of vesicle buffer were added in that order without mixing. A SW55Ti rotor (Beckman) was used for gradient centrifugation at 280,000 × *g* for 150 min at 4 °C. Vesicle-bound large α-Syn oligomers were recovered from the range between 0% and 30% histodenz. The amounts of large α-Syn oligomers, compared with the initial input of α-Syn, were measured by Western blot.

Western Blot. Purified proteins were applied to 15% SDS/PAGE and then transferred to PVDF membrane (Bio-Rad), which was blocked by 5% (wt/wt) skim milk solution for 1 h and incubated with the α-Syn primary antibody [sc-52979 (Santa Cruz Biotechnology), 1:750 dilution factor] for 5 h at room temperature. The membrane was washed with TBST buffer (500 mM Tris, pH 8.5; 150 mM NaCl; 0.05% Tween-20), incubated with anti-mouse IgG peroxidase secondary antibody (Sigma; 1:2,500 dilution factor), washed again with TBST buffer, and reacted with chemiluminescent substrate solution (Thermo SuperSignal West Pico Chemiluminescent Substrate). The bands were detected using LAS-4000 (Fujifilm Life Science).

Transmission Electron Microscopy. Purified large α-Syn oligomers were loaded on a 300-mesh copper grid (Electron Microscopy Sciences) and negatively stained with 2% uranyl acetate. The images were obtained with a JEM-1011 transmission electron microscope (JEOL).

Preparation of SNARE Proteins and Proteoliposome Reconstitution. His6×-tagged syntaxin-H_{abc}-truncated (amino acids 168–288; two cysteines were replaced with alanines) was cloned into pET28-a, and GST-tagged synaptosomal-associated protein-25 (SNAP-25) (amino acids 1–206; four cysteines were replaced with alanines), synaptobrevin-2 (amino acids 1–116; one cysteine was replaced with alanine), and N-terminal truncated mutant of synaptobrevin-2 (nt-synaptobrevin-2, amino acids 29–116) were cloned into pGEX-KG, respectively. *Escherichia coli* BL21 Rosetta (DE3) pLysS (Novagene) was used for protein expression. The detailed procedures of protein purification have been described well elsewhere (4).

POPC, DOPS, and Chol (Avanti Polar Lipids) were used to form liposomes. DiI and DiD were used as FRET donor and acceptor dyes, respectively (Invitrogen). The molar ratio of POPC:DOPS:Chol:DiI (or DiD) = 71:7:20:2 was used for both t-vesicle (DiI) and v-vesicle (DiD). The procedures for preparing proteoliposomes were described elsewhere (5), and

the size of proteoliposomes was measured by dynamic light scattering.

In Vitro Lipid-Mixing Assay. Two populations of proteoliposomes, t-vesicles doped with DiI and v-vesicles doped with DiD, were mixed together to form a 20-μM lipid concentration in the presence of α-Syn monomer or large oligomers and a 55-μL final reaction volume at 35 °C (Fig. 1*C*). We used the 532-nm wavelength for excitation and detected the signal at the wavelength of 690 nm as the FRET signal every 10 s using a temperature-controlled fluorescence spectrophotometer (Cary Eclipse, Varian). To study the interaction between large α-Syn oligomers and vesicle lipids (Fig. 2*A*), we prepared protein-free vesicles (**F**), the lipid composition of which is identical to that of t-vesicles except for the absence of fluorescent dyes. The size of the protein-free vesicles was similar to those of reconstituted proteoliposomes (50 nm in diameter).

Single-Vesicle Lipid-Mixing Assay by Alternating-Laser Excitation. The instrumental setup and the data analysis procedure of alternating-laser excitation (ALEX) were described previously (5). Briefly, for the single-vesicle lipid-mixing assay, t- and v-vesicles (20 μM final lipid concentration) were mixed with α-Syn in vesicle buffer (25 mM Hepes, pH 7.4, and 100 mM KCl) and then incubated for 30 min at 35 °C, the same condition as that of the bulk FRET assay. Then, the mixture was diluted three times with the same buffer, and the ALEX measurement was performed (10-min data collection). In ALEX, two lasers, one for donor dye excitation and the other for acceptor dye excitation, are focused tightly to excite only a femtoliter volume (Fig. 3*A*). When vesicle samples are diluted enough (as low as 100 pM vesicle concentration), only one vesicle passes through the excitation volume. This diffusing-in-and-out event of a vesicle through the excitation volume generates a fluorescent burst, as shown in the time traces (Fig. 3*B*). Because two lasers are alternated faster than the diffusing time of a vesicle passing through the excitation volume, three different types of fluorescence emissions are obtained from each vesicle (6). I_D^D is the fluorescent emission of the donor dye excited by the donor-excitation laser, I_D^A the fluorescent emission of the acceptor dye excited by the donor-excitation laser (a FRET signal), and I_A^A the fluorescent emission of the acceptor dye excited by the acceptor-excitation laser (Fig. 3*B*). These three intensities of a vesicle are used to calculate two parameters, $\boldsymbol{E}$ (FRET efficiency) and $\boldsymbol{S}$ (stoichiometry ratio or sorting number):

$$E = \frac{I_D^A}{I_D^D + I_D^A} \text{ and } S = \frac{I_D^D + I_D^A}{I_D^D + I_D^A + I_A^A}.$$

It should be noted that the unreacted vesicle, the docked-but-unfused vesicle, and the lipid-mixed vesicle have different sets of $\boldsymbol{E}$ and $\boldsymbol{S}$ values (Fig. 3*C*). For example, the unreacted t-vesicle doped with the donor dye has $I_A^A \approx 0$ and $I_D^A \approx 0$, because it does not have the acceptor dye. The t-vesicle has $\boldsymbol{E} = 0$ and $\boldsymbol{S} = 1$. In the same manner, the unreacted v-vesicle doped with the acceptor dye has $I_D^D \approx 0$ and $I_D^A \approx 0$ (no donor dyes), which results in $\boldsymbol{E}$ = determined by the background signal and $\boldsymbol{S} = 0$. In cases in which both the docked-but-unfused and the lipid-mixed vesicles have both donor and acceptor dyes ($I_D^D + I_D^A \approx I_A^A$), their $\boldsymbol{S}$ values become 0.5. Then, the docked-but-unfused and the lipid-mixed vesicles are discriminated by $\boldsymbol{E}$. Typically, the docked vesicle has low $\boldsymbol{E}$, whereas the lipid-mixed vesicle has high $\boldsymbol{E}$ because of lipid mixing (7). Thus, the docked vesicle has $\boldsymbol{E}$ = low and $\boldsymbol{S}$ = 0.5, whereas the lipid-mixed one has $\boldsymbol{E}$ = high and $\boldsymbol{S}$ = 0.5. As a result, the bursts of unreacted, docked, and lipid-mixed vesicles appear at the different regions in the $\boldsymbol{E}$–$\boldsymbol{S}$ graph (Fig. 3).

For the analysis of the fraction of lipid-mixed vesicles, we graphically selected vesicle numbers from the $\boldsymbol{E}$–$\boldsymbol{S}$ graph as before (5). For this analysis, we used an "acceptor photon search" to search the docked-but-unfused vesicles, lipid-mixed vesicles, and unreacted v-vesicles with the same efficiency (Fig. S8). Then we counted the number of bursts selected graphically using the $\boldsymbol{E}$–$\boldsymbol{S}$ graph: $0.15 < \boldsymbol{S} < 0.75$ and $0 < \boldsymbol{E} < 0.5$ for docked vesicles, $0.25 < \mathrm{S} < 1$ and $0.5 < \mathrm{E} < 1$ for lipid-mixed vesicles, and the rest for unreacted v-vesicles (Fig. S8).

Cell Viability. Cell viability was determined using a modified MTT [3-(4,5-dimethylthiazol-2-yl)-2,5-diphenyltetrazolium bromide] assay. Briefly, cells in the exponential growth phase were harvested by trypsinization, seeded at a concentration of 2×10^5 cells per well on 24-well plates, and allowed to stand overnight for attachment. Following α-Syn protein transfection, the MTT solution was added to each well with 1/5 volume of media. After incubation for 3 h at 37 °C in the dark, absorbance at 570 nm was measured by a multiwell plate reader. For each treatment, the cell viability was evaluated as a percentage using the following equation: (A_{570} of α-Syn–treated sample/A_{570} of untreated sample) × 100.

1. Volles MJ, et al. (2001) Vesicle permeabilization by protofibrillar alpha-synuclein: Implications for the pathogenesis and treatment of Parkinson's disease. *Biochemistry* 40(26):7812–7819.
2. Volles MJ, Lansbury PT, Jr. (2002) Vesicle permeabilization by protofibrillar alpha-synuclein is sensitive to Parkinson's disease-linked mutations and occurs by a pore-like mechanism. *Biochemistry* 41(14):4595–4602.
3. Takamori S, et al. (2006) Molecular anatomy of a trafficking organelle. *Cell* 127(4):831–846.
4. Kweon DH, Kim CS, Shin YK (2003) Insertion of the membrane-proximal region of the neuronal SNARE coiled coil into the membrane. *J Biol Chem* 278(14):12367–12373.
5. Kim JY, et al. (2012) Solution single-vesicle assay reveals PIP_2-mediated sequential actions of synaptotagmin-1 on SNAREs. *EMBO J* 31(9):2144–2155.
6. Kapanidis AN, et al. (2004) Fluorescence-aided molecule sorting: Analysis of structure and interactions by alternating-laser excitation of single molecules. *Proc Natl Acad Sci USA* 101(24):8936–8941.
7. Weber T, et al. (1998) SNAREpins: Minimal machinery for membrane fusion. *Cell* 92(6): 759–772.

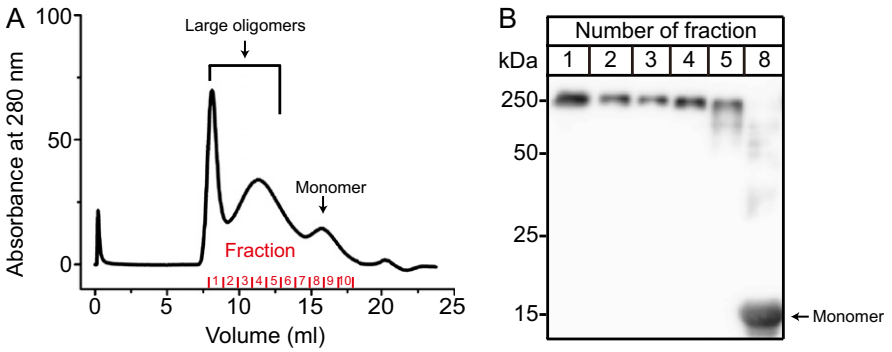

Fig. S1. Purification of dopamine-induced large α-Syn oligomers by size exclusion chromatography. (*A*) Elution profile of α-Syn after incubation with 100 μM dopamine for 72 h. A Superdex 200 10/300 GL column was used. Each elution fraction (1 mL) was collected in separate tubes. (*B*) Western blot analysis of eluted large α-Syn oligomers. Each fraction collected from *A* was concentrated and applied to 15% SDS/PAGE. The Western blot image shows that from fractions 1 through 5, large α-Syn oligomers were major species, whereas fraction 8 contained mostly α-Syn monomers. For consistency of the measurements, we used large α-Syn oligomers only from fraction 1 for all experiments, including electron micrograph (Fig. 1*B*).

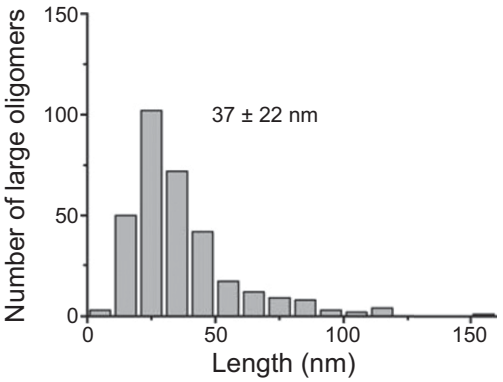

Fig. S2. Size distribution of large α-Syn oligomers measured by electron micrograph. The size (or length) of purified large α-Syn oligomers was analyzed by electron micrograph. A total of 326 particles from three independently prepared samples were used in this analysis. Each large oligomer was selected and measured manually using the ImageJ software. The average size of large α-Syn oligomers was 37 ± 22 nm.

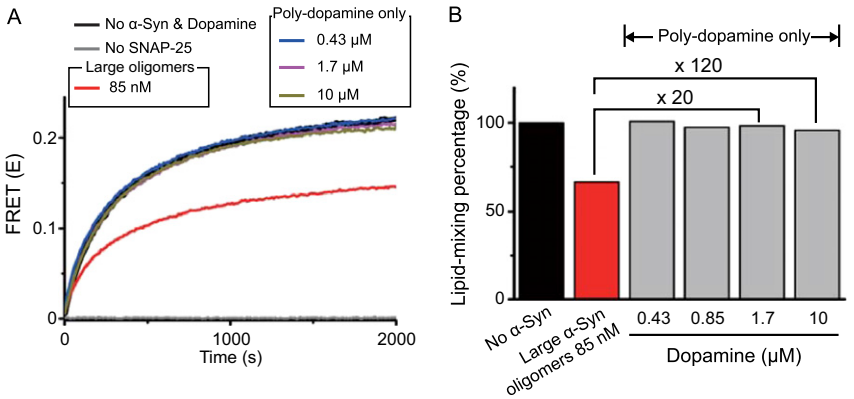

Fig. S3. The effect of polydopamine on lipid mixing. To investigate the effects of dopamine oxidants or polydopamine on lipid mixing, we added poly-dopamine to the lipid-mixing reaction. Polydopamine was prepared by incubating 100 μM dopamine without α-Syn proteins at 37 °C for 72 h. A recent study with large α-Syn oligomers generated by incubation with dopamine showed that dopamine-induced large α-Syn oligomers have a molar ratio of approximately 1:20 between α-Syn and dopamine (1). Thus, we added a 20-fold molar excess of polydopamine (1.7 μM by monomer unit) for large α-Syn oligomers (85 nM in monomer units), which showed no inhibitory effect (*A*). (*B*) We increased the amount of polydopamine further to more than 100-fold excess (10 μM), but there still was no inhibition of lipid mixing.

1. Rekas A, et al. (2010) The structure of dopamine induced alpha-synuclein oligomers. *Eur Biophys J* 39(10):1407–1419.

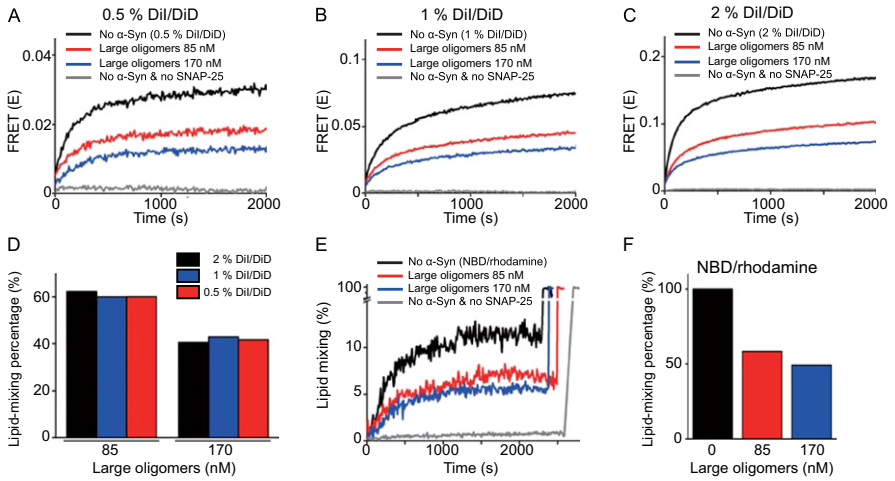

Fig. S4. Effects of fluorescent lipid dyes on inhibition of lipid mixing by large α-Syn oligomers (*SI Text*, *Fluorescent Lipid Dyes Have No Effect on the Inhibition of Lipid Mixing by Large α-Syn Oligomers*). (*A* and *B*) The concentration of the DiI/DiD pair in the vesicles was varied (*SI Text*). (*A*) 0.5% of DiI/DiD, (B) 1% of DiI/DiD, and (*C*) 2% of DiI/DiD (for the purpose of comparison, we used the same data from Fig. 1C). (*D*) FRET decrease with respect to the control with no α-Syn calculated from the results of *A*–*C*. A similar level of inhibition by large α-Syn oligomers was observed for different dye concentrations. (*E*) The NBD/rhodamine dye pair was used instead of the DiI/DiD pair. Here, NBD and rhodamine initially were incorporated into the v-vesicles. The fluorescence recovery of NBD initially quenched by 1.5% rhodamine in v-vesicles due to lipid mixing with dye-free t-vesicles was observed. (*F*) Relative fluorescence intensities of NBD in *E* at 1,800 s. The inhibition of lipid mixing by large α-Syn oligomers measured by NBD/rhodamine was similar to that measured by DiI/DiD.

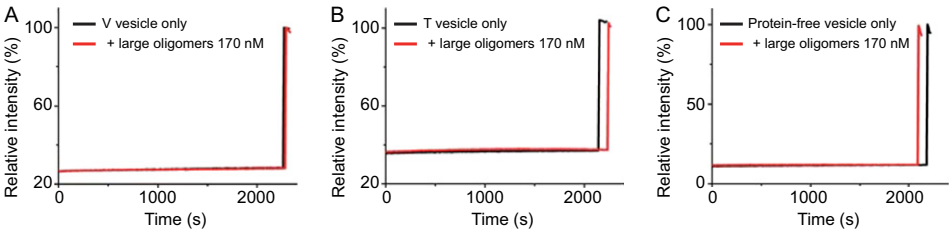

Fig. S5. Test of membrane disruption by large α-Syn oligomers (*SI Text*, *No Membrane Disruption Was Induced by Large α-Syn Oligomers*). SRB (20 mM) was encapsulated in vesicles in a fluorescently quenched state. Had the membrane been disrupted or permeabilized, SRB would have been released from the vesicles and we would have observed an increase in fluorescence. Vesicles (10 μM in lipids) encapsulating 20 mM SRB were mixed with 170 nM large α-Syn oligomers, then the intensities of the SRB fluorescence were monitored for more than 2,000 s at 35 °C: (*A*) v-vesicles, (*B*) t-vesicles, and (*C*) protein-free vesicles, respectively. At an appropriate time after 2,000 s, 0.1% Triton X-100 was added to the sample to break the vesicles and verify encapsulation of SRB. In all three cases, no disruption of the membrane was observed.

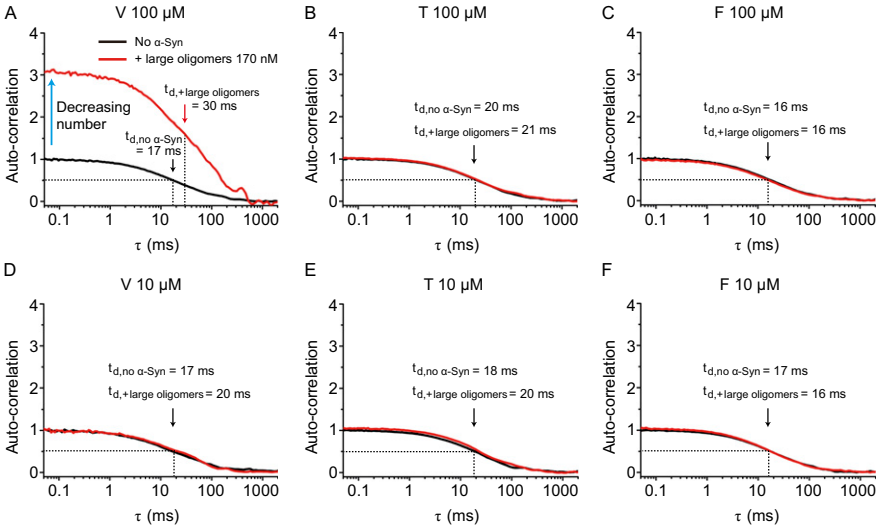

Fig. S6. Fluorescence correlation spectroscopy (FCS) measurement for v-vesicle clustering induced by large α-Syn oligomers. To examine whether large α-Syn oligomers cluster v-vesicles, we performed the FCS measurement (1). The vesicle clustering by large α-Syn oligomers would cause two changes (2): clustered vesicles would diffuse slower than unclustered vesicles in solution, and (3) the number of diffusing particles would be reduced. These two effects could be detected readily by the FCS measurement. We incubated the protein-free liposomes (F), t-vesicles (T), and v-vesicles (V), doped with 2% DiI, for 30 min at room temperature with/without 170 nM large α-Syn oligomers, respectively. Then, we performed the FCS measurement for each sample for 5 min and then the autocorrelation curve was obtained using the homemade LabVIEW analyzing program. (*A*–*C*) Autocorrelation curves obtained at the 100-μM lipid concentration: (*A*) v-vesicles, (*B*) t-vesicles, and (*C*) protein-free vesicles. The diffusion time (t_d) of the reconstituted vesicles in the absence of large α-Syn oligomers (black lines) was 16–20 ms (black ↓). The addition of large α-Syn oligomers to t-vesicles or the protein-free vesicles had no effect on the diffusion time (*B* and *C*, red lines). However, when large α-Syn oligomers were added to v-vesicles, the diffusion time of the vesicles increased significantly from 17 ms to 30 ms (*A*). At the same time, the amplitude of the autocorrelation curve increased (*A*), which implies that the particle number in solution decreased. These two changes clearly show that large α-Syn oligomers induce clustering of v-vesicles. (*D*–*F*) Autocorrelation curves obtained at the much reduced 10-μM lipid concentration: (*D*) v-vesicles, (*E*) t-vesicles, and (*F*) protein-free vesicles. When the vesicle concentration was reduced to the level of the single-vesicle detection, similar vesicle clustering by large α-Syn oligomers was not observed for all types of vesicles. The probability that large α-Syn oligomers interact with more than two vesicles simultaneously seems too low to induce vesicle clustering at the low vesicle concentration (10 μM in lipid concentration).

1. Cypionka A, et al. (2009) Discrimination between docking and fusion of liposomes reconstituted with neuronal SNARE-proteins using FCS. *Proc Natl Acad Sci USA* 106(44):18575–18580.
2. Rekas A, et al. (2010) The structure of dopamine induced alpha-synuclein oligomers. *Eur Biophys J* 39(10):1407–1419.
3. Volles MJ, et al. (2001) Vesicle permeabilization by protofibrillar alpha-synuclein: Implications for the pathogenesis and treatment of Parkinson's disease. *Biochemistry* 40(26): 7812–7819.

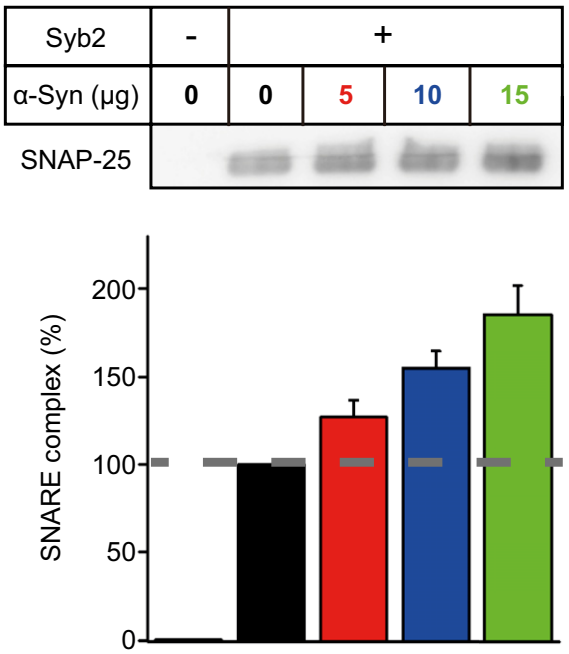

Fig. S7. α-Syn monomer promotes SNARE complex assembly in vitro. To investigate the effects of the α-Syn monomer on SNARE assembly, we used the coflotation assay as Südhof and coworkers (1) did previously. Briefly, 100 μM of proteoliposome reconstituted with synaptobrevin-2 (Syb2) was incubated with t-SNARE (syntaxin H3 and SNAP-25) in the presence or absence of the α-Syn monomer at 4 °C for 16 h in the dark. The lipid composition and the protein-to-lipid ratio of the vesicles were identical to those used in the in vitro lipid-mixing assays in Fig. 1. We separated the assembled SNARE complex by the coflotation method. The amounts of SNARE complex were measured by detecting SNAP-25 (*Upper*). As a negative control, liposome without Syb2 was incubated with t-SNARE (lane 1). To the mixture was added 0 μg (lane 2, black), 5 μg (lane 3, red), 10 μg (lane 4, blue), and 15 μg (lane 5, green) of the α-Syn monomer, respectively. The result clearly shows that the assembly of SNARE complex was promoted as the amount of the incubated α-Syn monomer was increased, which is consistent with the previous work (1). Bar graphs were obtained from three independent measurements.

1. Burré J, et al. (2010) Alpha-synuclein promotes SNARE-complex assembly in vivo and in vitro. *Science* 329(5999):1663–1667.

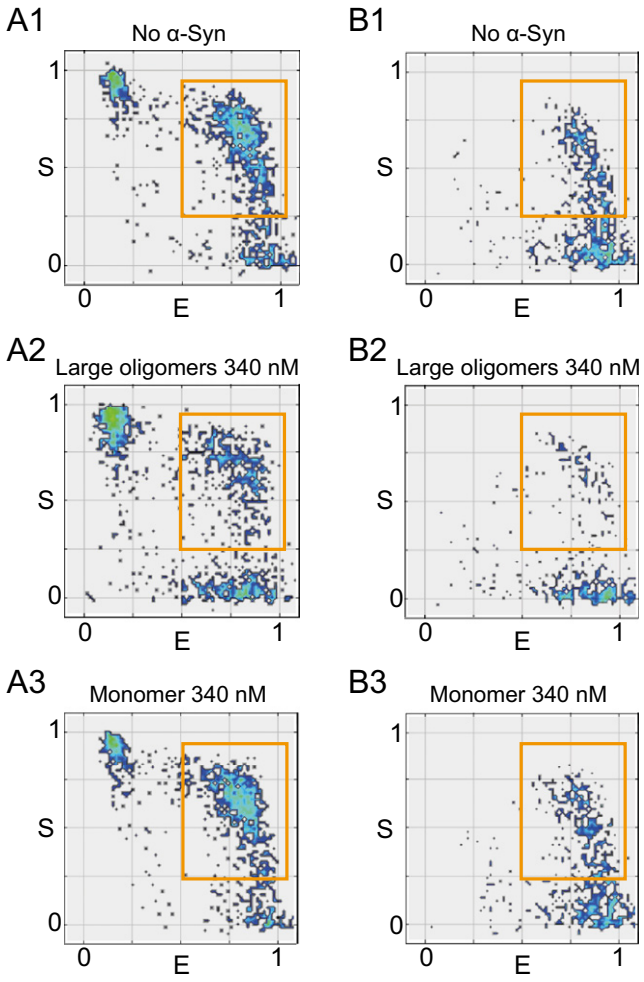

Fig. S8. Analysis of subpopulations from the ***E–S*** graph. For the presentation of the ***E–S*** graph, two burst search methods are used, i.e., "all photon search" and "acceptor photon search" (for details, see ref. 1). Briefly, "all photon search" is used to present all fluorescent species in reaction mixture (Fig. 3). However, this searching method selects docked and lipid-mixed vesicles, which contain both donor and acceptor dyes, more efficiently than unreacted vesicles. On the contrary, "acceptor photon search" provides quantitative measurement of the subpopulations of unreacted v-vesicles, docked vesicles, and lipid-mixed vesicles. Thus, we used "acceptor photon search" to measure the fraction of lipid-mixed vesicles. (*A1–A3*) ***E–S*** graphs obtained by "all photon search": (*A1*) no α-Syn (the same as Fig. 3*D*), (*A2*) 340 nM large α-Syn oligomers (the same as Fig. 3*E*), and (*A3*) 340 nM α-Syn monomer (the same as Fig. 3*F*). (*B1–B3*) ***E–S*** graphs obtained by "acceptor photon search"; these graphs were generated using the same data as *A1*, *A2*, and *A3*, respectively. We selected bursts (vesicles) graphically using the ***E–S*** graph and counted the number of bursts: $0.25 < S < 1$ and $0.5 < E < 1$ for lipid-mixed vesicles (orange box) and $0 < S < 0.25$ for unreacted v-vesicles.

1. Volles MJ, et al. (2001) Vesicle permeabilization by protofibrillar alpha-synuclein: Implications for the pathogenesis and treatment of Parkinson's disease. *Biochemistry* 40(26): 7812–7819.